COMPUTER METHODS AND PROGRAMS IN BIOMEDICINE 103 (2011) 113–120

journal homepage: www.intl.elsevierhealth.com/journals/cmpb

Scaling analysis of baseline dual-axis cervical accelerometry signals

Ervin Sejdić[a,c,*], *Catriona M. Steele*[b], *Tom Chau*[a]

[a] *Bloorview Research Institute, Holland Bloorview Kids Rehabilitation Hospital and the Institute of Biomaterials and Biomedical Engineering, University of Toronto, Toronto, Ontario, Canada*

[b] *Toronto Rehabilitation Institute and the Department of Speech-Language Pathology, University of Toronto, Toronto, Ontario, Canada*

[c] *Division of Gerontology, Beth Israel Deaconess Medical Center and Harvard Medical School, Harvard University, Boston, MA, USA*

ARTICLE INFO

Article history:
Received 27 October 2009
Received in revised form
6 April 2010
Accepted 23 June 2010

Keywords:
Dual-axis swallowing accelerometry signals
Scaling analysis
Detrended fluctuation analysis

ABSTRACT

Dual-axis cervical accelerometry is an emerging approach for the assessment of swallowing difficulties. However, the baseline signals, i.e., vibration signals with only quiet breathing or apnea but without swallowing, are not well understood. In particular, to comprehend the contaminant effects of head motion on cervical accelerometry, we need to study the scaling behavior of these baseline signals. Dual-axis accelerometry data were collected from 50 healthy adult participants under conditions of quiet breathing, apnea and selected head motions, all in the absence of swallowing. The denoised cervical vibrations were subjected to detrended fluctuation analysis with empirically determined first-order detrending. Strong persistence was identified in cervical vibration signals in both anterior–posterior (A–P) and superior–inferior (S–I) directions, under all the above experimental conditions. Vibrations in the A–P axes exhibited stronger correlations than those in the S–I axes, possibly as a result of axis-specific effects of vasomotion. In both axes, stronger correlations were found in the presence of head motion than without, suggesting that head movement significantly impacts baseline cervical accelerometry. No gender or age effects were found on statistical persistence of either vibration axes. Future developments of cervical accelerometry-based medical devices should actively mitigate the effects of head movement.

1. Introduction

The videofluoroscopic swallowing study (VFSS) is the current gold standard for the detection and management of dysphagia (swallowing difficulties) [1]. Nevertheless, VFSS is not suitable for ongoing monitoring due to excessive exposure to radiation, long waiting lists at hospitals and lack of availability in many communities [2,3]. In recent years, swallowing accelerometry has emerged as an alternative approach for non-invasive assessment of swallowing disorders [4,5]. Swallowing accelerometry is a technique involving the attachment of an accelerometer at the patient's neck. Traditionally, single-axis accelerometers were used [6–9]. However, it has been shown recently that dual-axis accelerometers yield more information and enhance diagnostic capabilities [10,11], likely as a result of the two-dimensional movement of the hyoid and the larynx during swallowing [12,13].

In previous contributions it has been noted that various phenomena, not related to swallowing, can alter the amplitude of swallowing accelerometry signals. These include small low-frequency vibrations observed in the baseline state (e.g., [14]) or head motion effects during swallowing (e.g., [10,11]). However, to the best of our knowledge, there are no contribu-

* *Corresponding author*. +1 416 425 6220x3515.
E-mail addresses: esejdic@ieee.org (E. Sejdić), steele.catriona@torontorehab.on.ca (C.M. Steele), tom.chau@utoronto.ca (T. Chau).
0169-2607/$ – see front matter © 2010 Elsevier Ireland Ltd. All rights reserved.
doi:10.1016/j.cmpb.2010.06.010

tions considering the effects of these phenomena on dual-axis swallowing accelerometry signals. In particular, given that the aforementioned contaminant signals lie in the low-frequency range and usually exist for the duration of a swallow, it is worthwhile to examine the scaling behaviour of swallowing accelerometry signals. Understanding such behaviour may help uncover age, gender or head motions effects on dual-axis swallowing accelerometry signals.

The main contributions of this paper are the exposure of strong statistical persistence in baseline dual-axis cervical vibration signals and the effects of demographic variables on such dependencies. Throughout this paper, "baseline" refers to dual-axis accelerometry signals collected at the neck during quiet breathing and apnea, in the absence of swallowing.

This paper is organized as follows: in the next section, we review the principles of scaling analysis and detrended fluctuation analysis. In Section 3, we describe the data collection and analysis methods. The results of the analysis are covered in Section 4 along with a discussion. Finally, conclusions are drawn in Section 5.

2. Mathematical background

Signals acquired by a dual-axis accelerometer are analyzed in this paper. Nevertheless, to avoid repetition, the discussion below is based on a signal acquired from a single-axis only. It should be noted, however, that the exact same analysis is conducted for both axes. Furthermore, we will assume that the acquired signals, $x(n)$, represent observations made during the time interval $0 \le n \le N-1$, where N represents the length of the signal. From the time series point of view, we can consider $x(n)$ to be a discrete-time series since the observations are made at fixed time intervals from the discrete set of times, Θ (with N representing the cardinality of Θ) [15]. The time series can then be taken as a realization of the family of real-valued random variables $\{\chi_n, n \in \Theta\}$ that are considered to be a stochastic process defined on a probability space [15].

2.1. Scaling analysis

Baseline dual-axis swallowing accelerometry signals can be wide-sense stationary processes [14]. If such a process is denoted by $\{\chi_n : n = 0, 1, \dots\}$ with mean, μ_χ, and variance, σ_χ^2, then its covariance function $\mathrm{cov}(\chi_n, \chi_{n+k})$ is independent of n for all integers k [16]. Furthermore, its autocorrelation function is then defined as

$$\rho_k = \frac{\mathrm{cov}(\chi_n, \chi_{n+k})}{\sigma_\chi^2} \tag{1}$$

Often, the analysis of a time series stemming from such processes assumes that observations made over a large time span are independent. This assumption is often violated in practice (e.g., [17,18]), and these lengthy time series can exhibit long-range dependence. Hence, it is desirable to understand whether acquired time series exhibit any short or long-range dependence (e.g., [19,20]). Consider the sum, Γ_s:

$$\Gamma_s = \sum_{k=1}^{s} \chi_k \tag{2}$$

where its variance is given by

$$\mathrm{var}(\Gamma_s) = s\sigma_\chi^2 + \sum_{i=1}^{s}\sum_{j \neq i} \mathrm{cov}(\chi_i, \chi_j) \tag{3}$$

with $s \in \mathbb{N}$.

The asymptotic behaviour of (3) can be used to differentiate two kinds of processes [17]. One group of processes is characterized by an autocorrelation function that decays exponentially fast [17,18]. Processes in this group include short-range dependent processes with Markov chains and auto-regressive moving average processes of finite order. The second group of processes is characterized by an autocorrelation function that exhibits a behaviour different from an exponentially decay, i.e., the correlation at very large lags can still be non-zero. In other words, a time series with long-range dependence exhibits a slowly decaying correlation that typically obeys a power-law function:

$$\rho_k \sim |k|^{-\gamma} \tag{4}$$

where k denotes correlation lags and $0 < \gamma < 1$, is the rate of decay. The long-range dependence of a time series implies that although correlations at large lags can be very small, their cumulative effect is not negligible.

Many empirical time series observe long-range dependence or persistence, manifesting as consecutive bursts of small or large values [21]. In the frequency domain, a process exhibiting long-range dependence has a spectral density of the form [22]:

$$s_x(\omega) \sim |\omega|^{-\zeta} \text{ as } \omega \to 0 \tag{5}$$

where $\zeta > 0$. On the other hand, a spectral density of a short-range dependent process remains finite as $\omega \to 0$.

So-called Hurst exponents (denoted by H) are often used to characterize the long-range dependence present in time series (please refer to [22,23] for an in-depth coverage of the topic and examples of various applications). The Hurst exponent can be related to the spectral density of long-range dependent processes given by (5), namely, $\zeta = 2H - 1$ as long as $0.5 < H < 1$ [22]. There are several methods for estimating the Hurst exponent such as rescaled range analysis, periodogram method, variance method, Whittle estimator, and wavelet based methods [22,23]. However, there has been little consistency in Hurst exponent estimates across the different methods [24]. The discrepancy in the results indicate potential difficulties in applying Hurst estimators to experimental data obtained from physical processes. An additional problem arises if the given process contains multiple scaling exponents across different scaling regions. In this case, linear regression cannot be used to estimate the exponent over all scales. Doing so may yield a Hurst exponent estimate that grossly misrepresents the scaling behaviour. Furthermore, long-range dependence is associated with stationary processes [22], and hence some estimators implicitly assume stationarity. From previous studies, it is known that baseline dual-axis swallowing accelerometry signals can be stationary. Nevertheless, once these signals include swallows, they become nonsta-

tionary [11]. Hence, these traditional approaches for scaling estimation are not applicable, and an alternative approach is needed.

2.2. *Detrended fluctuation analysis*

Detrended fluctuation analysis (DFA) is a scaling analysis method developed to address the aforementioned shortcomings of other scaling methods. DFA uses a scaling exponent α to represent the (auto-)correlation properties of a time series and permits detection of statistical persistence behaviour embedded in nonstationary time series [25,26]. Furthermore, DFA avoids detection of long-range correlations that are an artifact of nonstationarity [27,28].

The algorithm for DFA has been outlined in previous contributions (e.g., [25–28]). Here, we only summarize the main steps. Given the noisy discrete-time observations of a signal, $x(n)$, of length N, the first step is to evaluate the cumulative sum of the signal. Then, the integrated series is divided into L non-overlapping segments of equal length, M. As outlined in Section 3.2, one should carefully choose values of M. As the next step, a local trend for each of the segments is calculated by a least-square fit of the data. Various polynomial orders such as linear, quadratic, cubic, or higher order polynomials can be used in the fitting procedure. Then, the variance around the local trend is determined. An increasing value of M will inherently produce an increasing value of $\Omega(M)$ due to the fact that longer segments can introduce greater deviations from a local trend. Therefore, DFA models fluctuations which scale with segment length, M, in a power-law fashion, independent of external trends and signal amplitude, i.e.,

$$\Omega(M) \propto M^{\alpha} \tag{6}$$

where α is the slope of the line observed in the log–log representation of $\Omega(M)$ versus M.

Given that the scaling exponent is typically estimated as the slope of a single line on a log–log plot of fluctuations versus scale, the presence of multiple scaling effects can yield inaccurate results. This crossover phenomenon (e.g., [27,29]) usually arises due to changes in the correlation properties of the signal at different temporal or spatial scales [30]. Therefore, extracting the global exponent can be misleading in the presence of crossover phenomena, and modifications to the DFA should be used (e.g., [31]). α can be related to correlation properties of a time series and in some cases to (4), such that $\gamma = 2 - 2\alpha$ [25,32,33]. Furthermore, α can be related to ζ value from the power spectral density defined in (5) as $\zeta = 2\alpha - 1$. From this relationship, it is clear that α is also related to the Hurst exponent. In fact, $\alpha = H$ for $0 \leq H \leq 1$ and $\alpha = H + 1$ for $H > 1$ [34–36]. From a physical point of view, the value of α has a specific meaning. In particular, there is no correlation present in a time series when $\alpha = 0.5$, i.e., the time series is white noise [25]. For $\alpha > 0.5$ it can be stated that the time series are positively correlated and for $\alpha < 0.5$ the time series is anticorrelated [27,37]. In addition, two special cases have been pointed out in the literature: $\alpha = 1$ indicates $1/f$ noise, while $\alpha = 1.5$ indicates Brownian noise [38]. A very popular description of the meaning of α is that it denotes the "roughness" of a time series. Higher values of α denote smoother time series (for example, $\alpha = 0.5$ for the white Gaussian noise which is considered very rough, while $\alpha = 1.5$ for the Brownian motion, which is considered very smooth) [38].

3. Methodology

Potential participants completed a short survey outlining his/her medical history. Participants were excluded if they had any known or prior symptoms of swallowing difficulties, or had a history of stroke or other neurological conditions, head or neck cancer, neck or spinal injury or a tracheostomy. Fifty consenting healthy adults (18–65 years of age, 26 females) participated in this study. Participants were purposefully recruited such that 4 different age ranges, i.e., 18–34, 35–44, 45–54, and 55–65 were proportionally represented. The research ethics board of Holland Bloorview Kids Rehabilitation Hospital (Toronto, Ontario, Canada) approved the study protocol and all participants provided signed consent.

Participants were seated comfortably in a chair. A dual-axis accelerometer (ADXL322, Analog Devices) was placed on the neck of each participant anterior to the cricoid cartilage and secured with double-sided tape. The two axes were positioned in the anterior–posterior (A–P) and superior–inferior (S–I) directions. Three additional sensors complemented the dual-axis accelerometry measurements and confirmed that the participants were indeed following the data collection protocol properly. In particular, we collected signals from a triple-axis accelerometer (MMA7260Q, SparkFun Electronics) attached to a headband and centred on the participant's forehead to monitor head motions; a respiratory belt (1370G, Grass Technologies) secured around the participant's diaphragm to monitor breathing patterns; and a microphone placed around 30 cm from the participant's mouth to capture vocalizations. The signals acquired from the dual-axis accelerometer were processed in hardware using a band-pass filter and an amplifier (P55, Grass Technologies). The pass band of the filter was set to 0.1–3000 Hz. The sampling frequency of 10 kHz was used to collect the amplified sensor data using a LabVIEW program running on a computer. The data were stored on the hard drive for subsequent analyses. Data collection from all the sensors was synchronized in time. The experimental setup is shown in Fig. 1.

The data collection procedure included seven primary tasks that were completed by each participant:

1. Remain silent and motionless for 60 s.
2. Remain silent, motionless and stop respiration for 10 s.
3. Remain silent and tilt head to the left 10 times.
4. Remain silent and tilt head to the right 10 times.
5. Remain silent and tilt head downward (infero-anterior to natural position) 10 times.
6. Remain silent and tilt head backward (infero-posterior to natural position) 10 times.
7. Remain silent and rotate head from right to left 5 times, and from left to right 5 times.

All participants were advised to refrain from swallowing during each task, but were permitted to swallow accumulated saliva between successive steps.

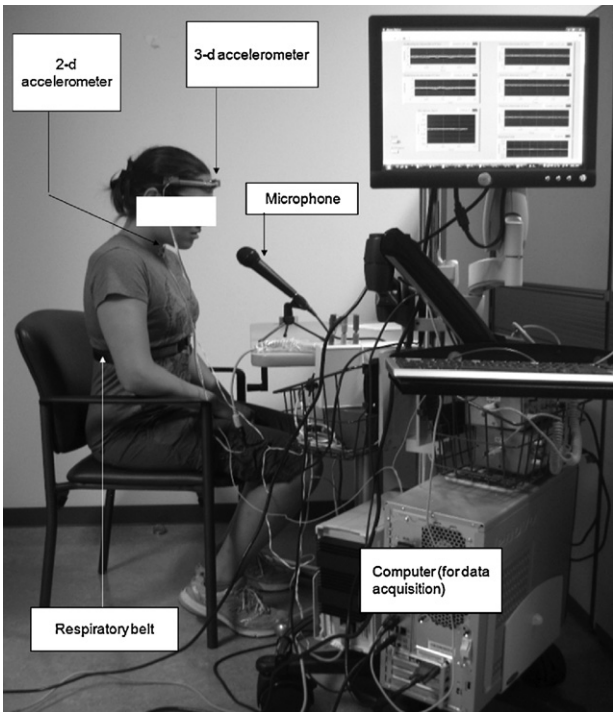

Fig. 1 – Instrumentation used for data collection in this study.

3.1. *Data analysis*

Using non-parametric significance tests (e.g., the Mann–Whitney test [39]), we checked for differences in statistical persistence between the A–P and S–I directions for the baseline dual-axis accelerometry signals. Furthermore, we investigated possible demographic effects on those correlations. In this paper, a 5% statistical significance level was used.

Prior to statistical analysis, the acquired signals were preprocessed with the inverse filters developed in [14]. The filtered signals were then denoised using a 10-level discrete wavelet transform using the discrete Meyer wavelet with soft thresholding [40,41]. DFA was carried out using the minimal and maximal values of the analyzing window and the order of the fitting polynomial, recommended in the following subsection.

3.2. *Initialization of DFA for dual-axis swallowing accelerometry signals*

There are three parameters in DFA: the smallest window size over which fluctuations are estimated, what we term the lower cutoff value, M_{min}; the largest window size over which fluctuations are estimated, what we term the upper cutoff value, M_{max}; and the order of the fitting polynomial. First, we consider how the analysis boundaries, M_{min} and M_{max}, are chosen. It has been suggested that very large M_{max} are preferred in order to deal with possibly very long correlations [26]. Nevertheless, as M_{max} approaches N the error in the estimation of α increases significantly. The ratio M_{max}/N represents the number of statistically independent measurements by which the value $\Omega(M)$ is obtained and the error associated with the estimation of α is inversely proportional to the square root of this ratio [26]. In particular, the standard deviation of α is given by [26,42]:

$$\sigma_\alpha \cong 0.1\sqrt{\frac{M_{max}}{N}} \tag{7}$$

Hence, the goal in the analysis of any type of signals is to have σ_α significantly smaller than the differences due to the phenomena of interest. It has been empirically observed that $M_{max} = N/10$ provides satisfactory results [26,27], which provides $\sigma_\alpha \approx 0.03$. Unfortunately, analogous guidelines for choosing the lower cutoff value are not available. It has been suggested that M_{min} should be chosen such that Markovian correlations do not affect the estimation of α [26]. Hence, different values for the lower cutoff value have been used in different applications. In some cases, the lower cutoff value is only a few data points (e.g., [37]). Nonetheless, for the scaling analysis of swallowing signals, we implemented a lower cutoff value of $M_{min} = N/100$. This value enables us to analyze signals over a decade of window sizes. Due to the fact that the error in the estimation of α increases proportionally with window size, a signal dependent rather than fixed upper cut off value was implemented (i.e., $M_{max} = N/10$). Hence, the window lengths used in the analysis were given by the following set of values:

$$\mathcal{M} = \left\{ M : M \in \mathbb{N} \text{ and } \left\lfloor \frac{N}{100} \right\rfloor \le M \le \left\lfloor \frac{N}{10} \right\rfloor \right\} \tag{8}$$

where the set contains fifty points equally spaced on a logarithmic scale. Hence, the set $\mathcal{M}$ provided us with a sufficient number of points to carry out an accurate fitting of a local trend.

The order of the fitting polynomial depends on the characteristics of the signals under analysis. A first-order polynomial was used for dual-axis cervical signals considered in this paper. To understand this particular choice, let's consider cumulative sum of a sample signal shown in Fig. 2(a), representing baseline vibrations in the A–P direction. The signal is divided into segments of the longest window size (i.e., a window with its length equal to $N/10$). Polynomial fitting using first, second and third orders are shown in Fig. 2(b)–(d), respectively. These figures depict that the local trend (thick solid line) is most accurately modeled by a first-order polynomial. Higher order polynomials tend to overfit the local trend. Therefore, for the rest of the analysis, a first-order polynomial was used to model local trends.

4. Results and discussions

Table 1 summarizes α values for signals in both A–P and S–I directions. A number of observations are in order. The statistical persistence observed in the A–P and the S–I directions are statistically different in all cases ($p \ll 0.01$), except for Test 3 ($p = 0.61$). α values in the A–P direction are higher than those in the S–I directions denoting stronger correlations. These results resonate with the findings of [14], which reports that the peak frequencies of the small vibrations associated with

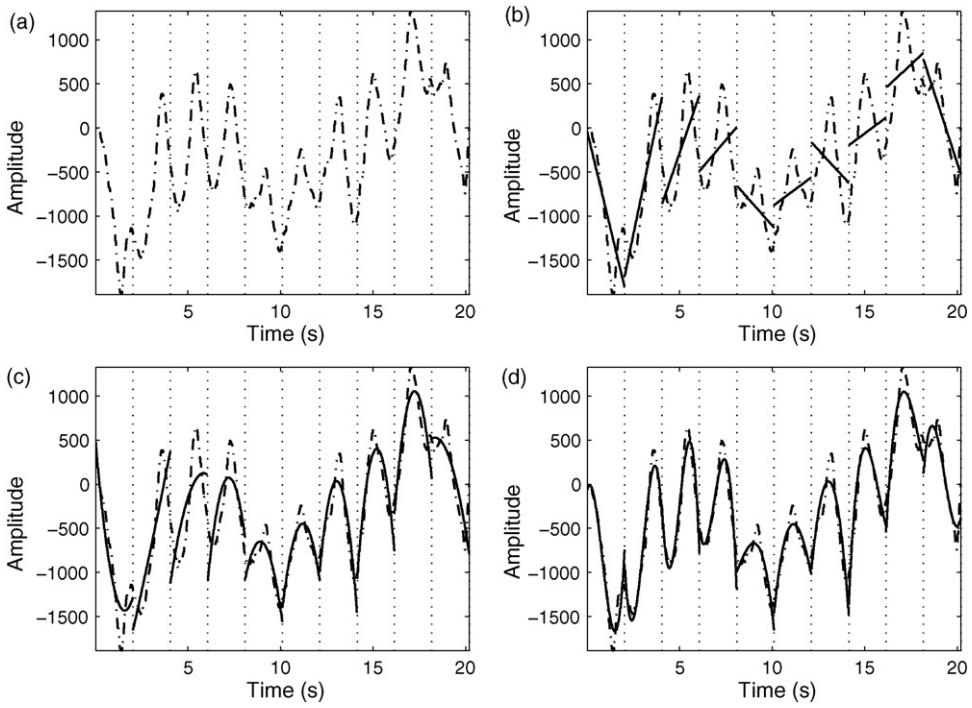

Fig. 2 – Choice of polynomial order for detrending in DFA. Cumulative sum of a sample cervical accelerometry signal is depicted in (a). Subsequent graphs show polynomial fits (solid line): (b) first-order; (c) quadratic; (d) third-order.

vasomotion near the thryroid cartilage are lower in the A–P direction than those in the S–I direction.

Hence, the vibrations in the A–P direction are dominated by low-frequency components indicative of strong statistical persistence. Observations should be also made regarding the effect of head position. In the A–P direction, the α values were statistically equal when considering all head tilting (Tests 3–6, $p = 0.46$, Kruskal–Wallis test). For both directions, higher α values are observed in tasks involving head movements (Tests 3–7) than in tasks without head motion (Tests 1 and 2). In the S–I direction, head movements induced statistically equivalent persistence for Tests 5 and 6 (Mann–Whitney test, $p = 0.77$). The results from both directions suggest that similar head positions (or movements) induced vibrations with similar statistical characteristics in the dual-axis cervical accelerometry signals. These results confirm findings from previous publications (e.g., [10,11]), which noted that head movements can significantly alter the amplitudes of dual-axis accelerometry signals.

Table 1 – Direction-based differences in α values.

Test	Overall	
	A–P	S–I
1. Motionless and quiet breathing	1.30 ± 0.18	1.11 ± 0.31
2. Motionless and apnea	1.08 ± 0.27	0.63 ± 0.24
3. Tilt head left	1.40 ± 0.20	1.39 ± 0.25
4. Tilt head right	1.42 ± 0.17	1.27 ± 0.23
5. Tilt head down	1.46 ± 0.19	1.14 ± 0.31
6. Tilt head back	1.42 ± 0.19	1.16 ± 0.23
7. Head rotation	1.52 ± 0.15	1.42 ± 0.22

It has been previously observed that there are no gender-based differences in the frequency content of cervical accelerometry signals [14]. As shown in Table 2, our analysis resonates with this previous finding. There are no gender-based differences in α values in either the A–P ($p > 0.34$) or S–I ($p > 0.23$) directions. However, within each gender, statistical differences generally exist between α values in the A–P and S–I directions ($p < 0.02$). The only exception occurs when considering Test 3 ($p > 0.44$) for both genders, where the α values are statistically equal between the A–P and S–I directions. Also, Test 7 ($p = 0.24$) for male participants and Test 4 ($p = 0.08$) for female participants have statistically equal α values for the A–P and S–I directions, likely due to the high variability of the α values for these two tests.

Tables 3 and 4 group α values according to age for the A–P and S–I directions, respectively. The α values in the S–I direction are statistically different from the α values in the A–P direction for all age groups. Furthermore, a linear regression revealed no dependence of α values on age in the A–P direction for Tests 1–6 ($p > 0.08$). These results are in accordance with those presented in [14], which showed that the baseline characteristics of dual-axis swallowing accelerometry signals are not statistically associated with the age or gender of participants.

Nevertheless, several interesting observations can be made about the statistical persistence of the cervical signals in the S–I direction (Tables 3 and 4). First, even though the regression analysis showed no age dependence, we observed that the mean α values increase with age for some of completed task.

In essence, higher α values denote stronger correlations (longer dependencies). Second, increasing α values with age

Table 2 – Gender-based differences in α values.

Test	Male		Female	
	A–P	S–I	A–P	S–I
1. Motionless and quiet breathing	1.28 ± 0.19	1.06 ± 0.38	1.32 ± 0.17	1.15 ± 0.25
2. Motionless and apnea	1.04 ± 0.26	0.61 ± 0.25	1.11 ± 0.29	0.66 ± 0.24
3. Tilt head left	1.42 ± 0.21	1.39 ± 0.27	1.38 ± 0.20	1.39 ± 0.23
4. Tilt head right	1.41 ± 0.18	1.25 ± 0.23	1.41 ± 0.17	1.29 ± 0.23
5. Tilt head down	1.45 ± 0.19	1.12 ± 0.38	1.46 ± 0.20	1.17 ± 0.24
6. Tilt head back	1.41 ± 0.19	1.11 ± 0.22	1.43 ± 0.19	1.20 ± 0.23
7. Head rotation	1.53 ± 0.15	1.44 ± 0.22	1.52 ± 0.16	1.39 ± 0.21

Table 3 – α variation in the A–P direction according to age of participants.

Test	$18 \leq$ Age < 35	$35 \leq$ Age < 45	$45 \leq$ Age < 55	$55 \leq$ Age < 65	p-Values
Test 1	1.26 ± 0.18	1.34 ± 0.16	1.32 ± 0.23	1.33 ± 0.12	0.14
Test 2	1.06 ± 0.28	1.05 ± 0.20	1.21 ± 0.26	0.96 ± 0.32	0.86
Test 3	1.34 ± 0.14	1.48 ± 0.21	1.36 ± 0.26	1.49 ± 0.18	0.28
Test 4	1.38 ± 0.14	1.48 ± 0.17	1.41 ± 0.17	1.43 ± 0.23	0.40
Test 5	1.42 ± 0.18	1.52 ± 0.20	1.52 ± 0.14	1.39 ± 0.25	0.55
Test 6	1.43 ± 0.21	1.43 ± 0.22	1.40 ± 0.18	1.43 ± 0.17	0.58
Test 7	1.49 ± 0.17	1.63 ± 0.10	1.52 ± 0.15	1.50 ± 0.13	0.43

Table 4 – α variation in the S–I direction according to age of participants.

Test	$18 \leq$ Age < 35	$35 \leq$ Age < 45	$45 \leq$ Age < 55	$55 \leq$ Age < 65	p-Values
Test 1	1.09 ± 0.31	1.15 ± 0.33	1.13 ± 0.34	1.04 ± 0.34	0.74
Test 2	0.60 ± 0.25	0.59 ± 0.27	0.68 ± 0.19	0.67 ± 0.29	0.33
Test 3	1.36 ± 0.27	1.49 ± 0.09	1.35 ± 0.32	1.43 ± 0.19	0.91
Test 4	1.32 ± 0.19	1.29 ± 0.14	1.21 ± 0.27	1.26 ± 0.32	0.27
Test 5	1.16 ± 0.23	1.11 ± 0.23	1.18 ± 0.30	1.08 ± 0.53	0.63
Test 6	1.18 ± 0.24	1.22 ± 0.16	1.07 ± 0.15	1.17 ± 0.40	0.73
Test 7	1.41 ± 0.21	1.49 ± 0.18	1.34 ± 0.24	1.44 ± 0.25	0.87

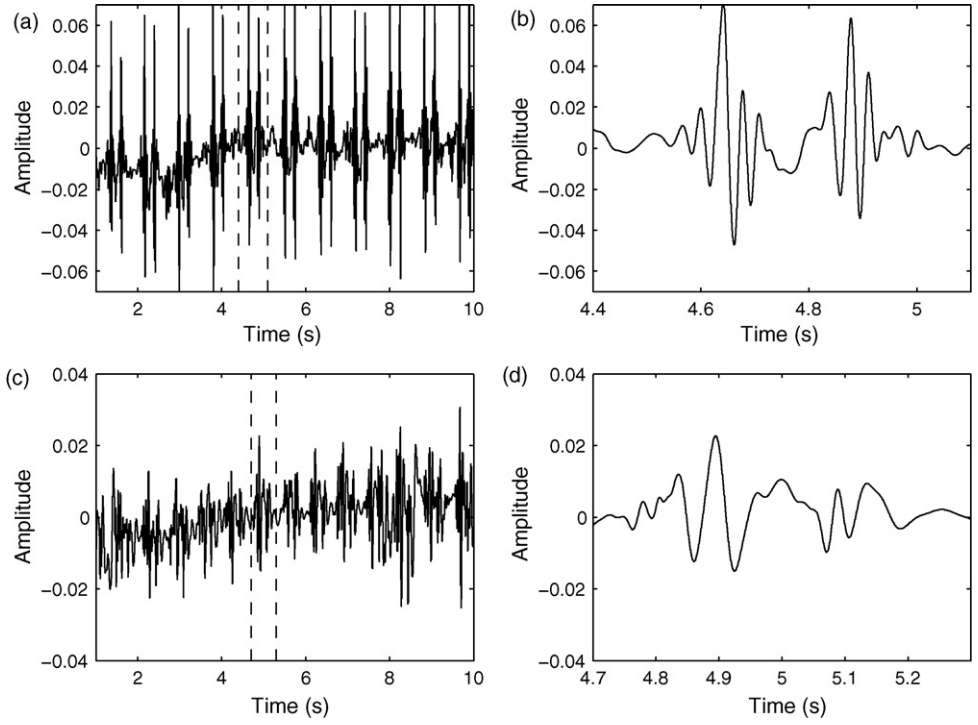

Fig. 3 – Cervical signals in the S–I direction during Test 1 from participants in two different age groups. A recording from a 19-year-old participant (a) and zoomed-in partition (b). A recording from a 65-year-old participant (c) and zoomed-in partition (d).

were observed regardless of whether or not the participants moved their heads (Tables 3 and 4, Tests 1–2 vs. Tests 3–7). This indicates that higher α values are not simply due to an age-related decrease in motor skills, but likely attributable in part to some other physiological/anatomical phenomena. A possible explanation for these observations stem from the age-related changes of human cardiovascular system. It is well known that human cardiac dynamics slow down with the age (e.g., [43,44]). Given that heart beats can be observed in these baseline recordings as shown in Fig. 3, we speculate that the age-related increases in α values are precisely due to slower cardiovascular dynamics. In other words, slower variations induce longer range dependencies. Differences in cardiac dynamics for participants from different age groups were also easily observed in Fig. 3(b) and (c). Younger participants have two strong components within each heart beat, while in older participants, the second component usually has decreased amplitude. Our speculations seem to align with the observations of [45], which analyzed cardiac interbeat interval dynamics using DFA. The authors also found higher α values in older participants, when considering cardiac time series up to approximately 30 heart beats, which was approximately the length of the time series considered in this paper.

5. Conclusion

In this paper, scaling analysis was conducted on baseline dual-axis cervical accelerometry signals in the absence of swallowing. We found that low frequency, small vibrations present in dual-axis cervical accelerometry signals introduced strong statistical persistence in these signals. Various head movements also had a strong influence on the long-range dependence of cervical accelerometry. Generally, the A–P axis experienced greater long-range dependence than the S–I axis. No gender-based differences were found in the observed long-range dependencies. Further developments of cervical accelerometry-based medical devices should account for head motion.

Acknowledgments

This research was funded in part by the Ontario Centres of Excellence, the Toronto Rehabilitation Institute, Bloorview Kids Rehab, and the Canada Research Chairs Program.

REFERENCES

[1] J.A. Logemann, Evaluation and Treatment of Swallowing Disorders, 2nd ed., PRO-ED, Austin, TX, USA, 1998.
[2] C. Steele, C. Allen, J. Barker, P. Buen, R. French, A. Fedorak, S. Day, J. Lapointe, L. Lewis, C. MacKnight, S. McNeil, J. Valentine, L. Walsh, Dysphagia service delivery by speech-language pathologists in Canada: results of a national survey, Canadian Journal of Speech-Language Pathology and Audiology 31 (4) (2007) 166–177.
[3] D.J.C. Ramsey, D.G. Smithard, L. Kalra, Can pulse oximetry or a bedside swallowing assessment be used to detect aspiration after stroke? Stroke 37 (December (12)) (2006) 2984–2988.
[4] N.P. Reddy, B.R. Costarella, R.C. Grotz, E.P. Canilang, Biomechanical measurements to characterize the oral phase of dysphagia, IEEE Transactions on Biomedical Engineering 37 (April (4)) (1990) 392–397.
[5] N.P. Reddy, E.P. Canilang, J. Casterline, M.B. Rane, A.M. Joshi, R. Thomas, R. Candadai, Noninvasive acceleration measurements to characterize the pharyngeal phase of swallowing, Journal of Biomedical Engineering 13 (September) (1991) 379–383.
[6] J. Lee, S. Blain, M. Casas, D. Kenny, G. Berall, T. Chau, A radial basis classier for the automatic detection of aspiration in children with dysphagia, Journal of NeuroEngineering and Rehabilitation 3 (July (14)) (2006) 17.
[7] T. Chau, D. Chau, M. Casas, G. Berall, D.J. Kenny, Investigating the stationarity of paediatric aspiration signals, IEEE Transactions on Neural Systems and Rehabilitation Engineering 13 (March (1)) (2005) 99–105.
[8] A. Das, N.P. Reddy, J. Narayanan, Hybrid fuzzy logic committee neural networks for recognition of swallow acceleration signals, Computer Methods and Programs in Biomedicine 64 (February (2)) (2001) 87–99.
[9] N.P. Reddy, A. Katakam, V. Gupta, R. Unnikrishnan, J. Narayanan, E.P. Canilang, Measurements of acceleration during videofluorographic evaluation of dysphagic patients, Medical Engineering and Physics 22 (July (6)) (2000) 405–412.
[10] E. Sejdić, C.M. Steele, T. Chau, Segmentation of dual-axis swallowing accelerometry signals in healthy subjects with analysis of anthropometric effects on duration of swallowing activities, IEEE Transactions on Biomedical Engineering 56 (April (4)) (2009) 1090–1097.
[11] J. Lee, C.M. Steele, T. Chau, Time and time-frequency characterization of dual-axis swallowing accelerometry signals, Physiological Measurement 29 (September (9)) (2008) 1105–1120.
[12] R. Ishida, J.B. Palmer, K.M. Hiiemae, Hyoid motion during swallowing: factors affecting forward and upward displacement, Dysphagia 17 (December (4)) (2002) 262–272.
[13] Y. Kim, G.H. McCullough, Maximum hyoid displacement in normal swallowing, Dysphagia 23 (September (3)) (2008) 274–279.
[14] E. Sejdić, V. Komisar, C.M. Steele, T. Chau, Baseline characteristics of dual-axis swallowing accelerometry signals, Annals of Biomedical Engineering 38 (March (3)) (2010) 1048–1059.
[15] P.J. Brockwell, R.A. Davis, Time Series: Theory and Methods, 2nd ed., Springer-Verlag, New York, NY, USA, 1991.
[16] A. Papoulis, Probability, Random Variables, and Stochastic Processes, 3rd ed., WCB/McGraw-Hill, New York, 1991.
[17] D.P. Heyman, T.V. Lakshman, What are the implications of long-range dependence for VBR-video traffic engineering? IEEE/ACM Transactions on Networking 4 (June (3)) (1996) 301–317.
[18] J. Beran, R. Sherman, M.S. Taqqu, W. Willinger, Long-range dependence in variable-bit-rate video traffic, IEEE Transactions on Communications 43 (February/March/April (2/3/4)) (1995) 1566–1579.
[19] A.H. Khandoker, S.B. Taylor, C.K. Karmakar, R.K. Begg, M. Palaniswami, Investigating scale invariant dynamics in minimum toe clearance variability of the young and elderly during treadmill walking, IEEE Transactions on Neural Systems and Rehabilitation Engineering 16 (August (4)) (2008) 380–389.
[20] D. Abásolo, R. Hornero, J. Escudero, P. Espino, A study on the possible usefulness of detrended actuation analysis of the electroencephalogram background activity in Alzheimer's disease, IEEE Transactions on Biomedical Engineering 55 (September (9)) (2008) 2171–2179.

[21] A. Erramilli, O. Narayan, W. Willinger, M. Bellcore, Experimental queuing analysis with long-range dependent packet traffic, IEEE/ACM Transactions on Networking 4 (April (2)) (1996) 209–223.
[22] K. Park, W. Willinger (Eds.), Self-Similar Network Traffic and Performance Evaluation, John Wiley, New York, NY, USA, 2000.
[23] G. Rangarajan, M. Ding (Eds.), Processes with Long-Range Correlations: Theory and Applications, Ser. Lecture Notes in Physics, Springer, Berlin, Germany, 2003.
[24] R.G. Kavasseri, R. Nagarajan, Evidence of crossover phenomena in wind-speed data, IEEE Transactions on Circuits and Systems I: Regular Papers 51 (November (11)) (2004) 2255–2262.
[25] C.-K. Peng, S.V. Buldyrev, S. Havlin, M. Simons, H.E. Stanley, A.L. Goldberger, Mosaic organization of DNA nucleotides, Physical Review E 49 (February (2)) (1994) 1685–1689.
[26] S.M. Ossadnik, S.V. Buldyrev, A.L. Goldberger, S. Havlin, R.N. Mantegna, K. Peng, M. Simons, H.E. Stanley, Correlation approach to identify coding regions in DNA sequences, Biophysical Journal 67 (July (1)) (1994) 64–70.
[27] Z. Chen, P.C. Ivanov, K. Hu, H.E. Stanley, Effect of nonstationarities on detrended fluctuation analysis, Physical Review E 65 (April (4)) (2002) 041107.
[28] M. Jospin, P. Caminal, E.W. Jensen, H. Litvan, M. Vallverdu, M.M.R.F. Struys, H.E.M. Vereecke, D.T. Kaplan, Detrended fluctuation analysis of EEG as a measure of depth of anesthesia, IEEE Transactions on Biomedical Engineering 54 (May (5)) (2007) 840–846.
[29] Z. Chen, K. Hu, P. Carpena, P. Bernaola-Galvan, H.E. Stanley, P.C. Ivanov, Effect of nonlinear filters on detrended fluctuation analysis, Physical Review E 71 (January (1)) (2005), 011104-1–011104-11.
[30] K. Hu, P.C. Ivanov, Z. Chen, P. Carpena, S.H. Eugene, Effect of trends on detrended fluctuation analysis, Physical Review E 64 (June (1)) (2001), 011114-1–011114-19.
[31] J.W. Kantelhardt, S.A. Zschiegner, E. Koscielny-Bunde, S. Havlin, A. Bunde, H.E. Stanley, Multifractal detrended fluctuation analysis of nonstationary time series, Physica A: Statistical Mechanics and its Applications 316 (December (1–4)) (2002) 87–114.
[32] J.W. Kantelhardt, E. Koscielny-Bunde, H.H.A. Rego, S. Havlin, A. Bunde, Detecting long-range correlations with detrended fluctuation analysis, Physica A: Statistical Mechanics and its Applications 295 (June (3–4)) (2001) 441–454.
[33] T. Penzel, J.W. Kantelhardt, L. Grote, J.H. Peter, A. Bunde, Comparison of detrended fluctuation analysis and spectral analysis for heart rate variability in sleep and sleep apnea, IEEE Transactions on Biomedical Engineering 50 (October (10)) (2003) 1143–1151.
[34] D. Delignieres, S. Ramdani, L. Lemoine, K. Torre, M. Fortes, G. Ninot, Fractal analyses for "short" time series: a re-assessment of classical methods, Journal of Mathematical Psychology 50 (December (6)) (2006) 525–544.
[35] F. Esen, H. Esen, Detrended fluctuation analysis of laser Doppler owmetry time series: the effect of extrinsic and intrinsic factors on the fractal scaling of microvascular blood flow, Physiological Measurement 27 (November (11)) (2006) 1241–1253.
[36] A. Eke, P. Herman, L. Kocsis, L.R. Kozak, Fractal characterization of complexity in temporal physiological signals, Physiological Measurement 23 (February (1)) (2002) R1–R38.
[37] R. Karasik, N. Sapir, Y. Ashkenazy, P.C. Ivanov, I. Dvir, P. Lavie, S. Havlin, Correlation differences in heartbeat fluctuations during rest and exercise, Physical Review E 66 (December (6)) (2002), 062902-1–062902-4.
[38] C.-K. Peng, S. Havlin, H.E. Stanley, A.L. Goldberger, Quantification of scaling exponents and crossover phenomena in nonstationary heartbeat time series, Chaos: An Interdisciplinary Journal of Nonlinear Science 5 (March (1)) (1995) 82–87.
[39] H.B. Mann, D.R. Whitney, On a test of whether one of two random variables is stochastically larger than the other, The Annals of Mathematical Statistics 18 (March (1)) (1947) 50–60.
[40] D.L. Donoho, De-noising by soft-thresholding, IEEE Transactions on Information Theory 41 (May (3)) (1995) 613–627.
[41] E. Sejdić, C.M. Steele, T. Chau, A procedure for denoising dual-axis swallowing accelerometry signals, Physiological Measurement 31 (January (1)) (2010) N1–N9.
[42] C.-K. Peng, S.V. Buldyrev, A.L. Goldberger, S. Havlin, M. Simons, H.E. Stanley, Finite-size effects on long-range correlations: Implications for analyzing DNA sequences, Physical Review E 47 (May (5)) (1993) 3730–3733.
[43] M. Brandfonbrener, M. Landowne, N.W. Shock, Changes in cardiac output with age, Circulation 12 (October (4)) (1955) 557–566.
[44] I.A. O'Brien, P. O'Hare, R.J. Corrall, Heart rate variability in healthy subjects: effect of age and the derivation of normal ranges for tests of autonomic function, British Heart Journal 55 (April (4)) (1986) 348–354.
[45] N. Iyengar, C.K. Peng, R. Morin, A.L. Goldberger, L.A. Lipsitz, Age-related alterations in the fractal scaling of cardiac interbeat interval dynamics, American Journal of Physiology: Regulatory, Integrative and Comparative Physiology 271 (October (4)) (1996) R1078–R1084.